PHYSICAL REVIEW B VOLUME 24, NUMBER 8 15 OCTOBER 1981

Determination of carrier densities in lightly doped silicon crystals from the Hall effect

A. Hackmann
Physikalisch-Technische Bundesanstalt, Institut Berlin,
Abbestrasse 2-12, D-1000 Berlin 10, Germany
and Institut für Theoretische Physik, Technische Universität Berlin,
Hardenbergstrasse 4-5, D-1000 Berlin 12, Germany

D. Neubert
Physikalisch-Technische Bundesanstalt, Institut Berlin, Abbestrasse 2-12,
D-1000 Berlin 10, Germany

U. Scherz
Institut für Theoretische Physik, Technische Universität Berlin,
Hardenbergstrasse 4-5, D-1000 Berlin 12, Germany

R. Schlief
Physikalisch-Technische Bundesanstalt, Institut Berlin,
Abbestrasse 2-12, D-1000 Berlin 10, Germany

(Received 24 March 1981)

The evaluation of carrier densities from the Hall effect depends very sensitively on the values of the Hall factors r_n and r_p. This sensitivity is particularly pronounced in the intermediate temperature region of *p*-type silicon crystals. This is due to the fact that there are generally two different carrier concentrations which lead to the same Hall coefficient. A general theory of Hall factors is presented, taking details of the band structure and phonon-scattering mechanisms of silicon crystals into account. A somewhat more stringent approach to the solution of the Boltzmann equation is used in this paper than that of taking the relaxation-time ansatz for granted. Of special importance is the third split-off valence band, which introduces an additional temperature dependence to the Hall factors. Problems connected with interpreting the solution of the Hall formula are examined and resolved. The theory is applied to measurements on lightly doped *n*- and *p*-type silicon single crystals with doping concentrations of about 10^{13} cm^{-3} in the temperature region between 90 and 450 K. The deformation-potential constants are determined and are found to be in fair agreement with previously published values.

I. INTRODUCTION

The concentration of free electrons n and free holes p are important parameters for the characterization of a semiconductor such as silicon, which is one of the most commonly used materials in modern solid-state electronics. In addition, from a theoretical point of view, silicon is one of the best-understood semiconductors and therefore an appropriate material for testing the current state of semiconductor theory.

The standard method for determining carrier concentrations is the measurement of the Hall coefficient R_H and the calculation of the carrier densities from this experimental quantity by use of the Hall formula[1-3]

$$R_H = -\frac{1}{e}\frac{b^2 r_n n - r_p p}{(bn+p)^2}\,, \tag{1}$$

where e is the electronic charge, r_n and r_p are the Hall factors for electrons and holes, respectively and $b=\mu_d^{(n)}/\mu_d^{(p)}$ is the ratio of electron drift mobility $\mu_d^{(n)}$ to hole drift mobility $\mu_d^{(p)}$.

In the extrinsic temperature region this formula reduces to the well-known and widely used form

$$R_H = -\frac{r_n}{en}\,,\quad R_H = \frac{r_p}{ep} \tag{2}$$

for n-type and p-type materials, respectively. In principle, the Hall factors r_n and r_p are temperature dependent and involve the details of band structure and scattering mechanisms. In practice, the Hall factors r_n and r_p are usually assumed to be independent of temperature and values such as $r_n = r_p = 1$ or $r_n = r_p = 3\pi/8$ are used. Since in Eq. (2), the Hall factor appears only as a multiplicative factor, one finds an acceptable carrier concentration independent of the accuracy of r_n and r_p. However, if one attempts to use the Hall formula, Eq. (1), for mixed conduction in the intrinsic and intermediate temperature region, one finds no satisfactory solution for the carrier densities. This has been previously pointed out by two of the authors.[4] They showed that the constant values $r_n = r_p = 3\pi/8$ as well as the temperature-dependent Hall factors given by Messier and Flores[5] lead to a surprising discontinuity in the temperature dependence of the hole density close to the intrinsic temperature region. Their result is shown in Fig. 9 of this paper. The reasons for this discontinuity are discussed in Sec. IV, where it is shown that the evaluation of carrier concentrations in this temperature region depends very sensitively on the correct values of the Hall factors. In addition, the difficulty connected with finding the true solution of the Hall formula, Eq. (1), is considered. This problem arises from the fact that in general two different carrier concentrations lead to the same Hall coefficient R_H. These considerations are similar to those discussed in the monograph by Putley[1] and are represented in graphical form similar to the well-known Dunlap ellipse.[1]

With respect to the problem of acceptable Hall factors r_n and r_p, a complete solution is still not yet available. Well-known treatises such as those by Beer[6] and Conwell[7] and the review articles by Rode[8] and Wiley[9] treat the principal aspects of transport theory and galvanomagnetic effects at a fundamental level, but they do not give the Hall factors in a sufficiently detailed and explicit form so that they can be used in routinely solving Eq. (1). Furthermore, compilations of silicon data, such as those by Wolf,[10] give no relevant information on the Hall factors. Thus, appropriate theoretical formulations for obtaining Hall factors in the intermediate and intrinsic temperature region are still necessary. Such calculations are considered in this paper and are given in Sec. II.

In Sec. II we shall calculate the transport coefficients for silicon for both the conduction and valence bands. In the simplest approach for spherical energy bands, electrons and holes are scattered by acoustic phonons with small wave vectors only, from which $r_n = r_p = 3\pi/8$ results.[1] In fact, in lightly doped silicon crystals (doping concentration $< 10^{16}$ cm^{-3}), impurity scattering is ineffective and phonon scattering is the main scattering mechanism. We consider two kinds of electronic transitions in the conduction band (cf. Herring and Vogt,[11] Herring,[12] and Conwell[7]): (a) intravalley acoustic-phonon scattering and (b) intervalley phonon scattering. In the valence band we consider the scattering of holes by acoustic and optical phonons. The transition probabilities resulting from these electron-phonon interactions are obtained by the deformation-potential method introduced by Bardeen and Shockley[13] and Meyer.[14] With respect to the specific band structure of silicon, we use for the conduction band the model of six equivalent ellipsoids in the Brillouin zone. The valence band is considered to consist of three spherical bands with different effective masses, one of which is split off by spin-orbit coupling. The coupling of the degenerate valence bands is also taken into account.

With these transition probabilities, the transport coefficients are obtained from the distribution functions as solutions of the Boltzmann equations. A somewhat more stringent approach to the solution of the Boltzmann equation is used in this paper than that of taking the relaxation time ansatz for granted. The integral equations which result from the Boltzmann equations are solved by expanding the distribution functions in terms of spherical harmonics. By taking only linear terms into account, these solutions may be written in terms of the relaxation-time formalism.

Our method leads to new results for the Hall factors r_n and r_p. The Hall factors become temperature dependent because of temperature dependent scattering mechanisms. For the valence band the temperature dependence is enhanced due to the split-off band.

The deformation potential constants are determined by fitting the theory to experimental results in Sec. III. Experiments have been performed in the temperature range 90–450 K at a magnetic induction $B_z = 1.3$ T for two single dislocation-free crystals with doping concentrations less than 10^{14} cm^{-3}. The deformation potential constants thus obtained are in fair agreement with values given by Murase *et al.*,[15] Costato and Reggiani,[16] and Wiley and DiDomenico.[17] With these deformation potential constants, the Hall factors r_n and r_p are calculated. It is shown that with these new values of r_n

and r_p it is still not possible to obtain a continuous carrier concentration in the intermediate temperature region. The fundamental underlying problem is discussed in Sec. V. It is hoped that this paper will contribute to a better understanding of a problem which at first sight appears to have been solved but which by closer examination is revealed to be largely unsolved in point of fact.

II. THEORY OF TRANSPORT COEFFICIENTS

In order to calculate the transport coefficients, we shall treat the conductivity tensor as a coupling parameter between current density $\vec{j}$ and electric field $\vec{E}$. In weak external fields, it is appropriate to expand the conductivity tensor with respect to the magnetic induction:

$$\vec{j}_j = \sum_{l=1}^{3} \sigma^0_{jl} E_l + \sum_{l,m}^{1,2,3} \sigma^0_{jlm} E_l B_m + \cdots \; . \tag{3}$$

Here $\vec{B}$ is the applied magnetic induction. The Hall coefficient R_H, with the cubic symmetry of the crystal taken into account,[18] may be written for small magnetic fields in the form given by Lax and Mavroides[19]:

$$R_H = \frac{\sigma^0_{123}}{(\sigma^0_{11})^2} \; . \tag{4}$$

The total homogeneous current density $\vec{j}$ in the sum is

$$\vec{j} = \sum_i \vec{j}^{(i)} \tag{5}$$

of the partial contributions $\vec{j}^{(i)}$ of the various energy bands i,

$$\vec{j}^{(i)} = \pm e \frac{2}{(2\pi)^3} \int \vec{v}^{(i)}(\vec{k}) f^{(i)}(\vec{k}) d\vec{k} \; , \tag{6}$$

with

$$\vec{v}^{(i)}(\vec{k}) = \frac{1}{\hbar} \vec{\nabla}_{\vec{k}} \epsilon^{(i)}(\vec{k}) \; ,$$

where $\vec{v}^{(i)}(\vec{k})$ is the carrier velocity, $\epsilon^{(i)}(\vec{k})$ is the energy of the band i, $2/(2\pi)^3$ is the density of states, and e is the electronic charge (+ sign for holes, − sign for electrons).

The central problem in transport theory is the determination of the distribution function $f^{(i)}(\vec{k})$ as a solution of the Boltzmann equations

$$\left[\frac{\partial f^{(i)}}{\partial t} \right]_{\text{field}} + \left[\frac{\partial f^{(i)}}{\partial t} \right]_{\text{coll}} = 0 \; . \tag{7}$$

If the bands are coupled, as in the case of the light- and heavy-hole band of Si, one has to solve a system of coupled Boltzmann equations.[20,21] The field term is given by

$$\left[\frac{\partial f^{(i)}}{\partial t} \right]_{\text{field}} = - \left[\pm \frac{e}{\hbar} \vec{E} \pm \frac{e}{\hbar} \vec{v}^{(i)} \times \vec{B} \right] \cdot \vec{\nabla}_{\vec{k}} f^{(i)}(\vec{k}) \; , \tag{8}$$

and the collision term is given by

$$\left[\frac{\partial f^{(i)}}{\partial t} \right]_{\text{coll}} = \frac{\Omega}{(2\pi)^3} \sum_j \int [W_{ji}(\vec{k}',\vec{k}) f^{(j)}(\vec{k}') - W_{ij}(\vec{k},\vec{k}') f^{(i)}(\vec{k})] d\vec{k}' \; . \tag{9}$$

For the case of the conduction band, the indices i and j are irrelevant, since this is an isolated band. The transition probability from the initial state $\vec{k}$ of band i to the final state $\vec{k}'$ of band j is denoted by $W_{ij}(\vec{k},\vec{k}')$; Ω is the volume of the crystal. In the collision term, the influence of the Pauli principle has not been taken into account. This is permissible under those conditions in which Boltzmann statistics can be applied.[22] The transition probabilities and the solution of the Boltzmann equation depend on the band structure.

In the following, we first consider the conduction band (Sec. II A) and then the valence band (Sec. II B). For each band, we first give the transition probabilities as taken from the literature and then use these transition probabilities to solve the Boltzmann equation and obtain the distribution function. Finally (Sec. II C), we present formulas for the various transport coefficients of interest.

A. Conduction band

The constant-energy surfaces for each of the six equivalent ellipsoids of the conduction band in Si are given by

$$\epsilon(\vec{k}) = \frac{\hbar^2}{2} \left[\frac{k_1^2}{m_1^*} + \frac{k_2^2}{m_2^*} + \frac{k_3^2}{m_3^*} \right] , \tag{10}$$

where m_i^*, $i = 1,2,3$, are the effective masses $m_\perp^*$ or $m_\parallel^*$, depending on the ellipsoid considered, with the numerical values given by Costato and Reggiani.[16]

1. Transition probabilities

The main scattering mechanism in pure Si is the phonon scattering. In the conduction band this mechanism produces three kinds of electronic transitions (cf. Herring and Vogt,[11] Herring,[12] and Conwell[7]:

(a) intravalley acoustic-phonon scattering,
(b) intervalley phonon scattering, and
(c) intravelley optical-phonon scattering.

It has been shown by Harrison[23] that process (c) is negligible in zeroth order. Furthermore in pure Si, impurity scattering is ineffective and shall be neglected.

The transition probability for acoustic-phonon scattering $W^{\mathrm{ac}}(\vec{k},\vec{k}')$ is given[7] by

$$W^{\mathrm{ac}}(\vec{k},\vec{k}')=\sum_{l=1}^{3}\frac{2\pi k_B T}{\hbar\Omega\rho\bar{v}^2}F_l^2(\theta)\,\delta(\epsilon(\vec{k}')-\epsilon(\vec{k}))\ , \tag{11}$$

where $F_l(\theta)$ are the following functions:

$$\begin{aligned} F_1(\theta)&=E_d+E_u\cos\theta\cos\theta\ ,\\ F_2(\theta)&=E_u\cos\theta\sin\theta\ ,\\ F_3(\theta)&=E_u\cos\theta\sin\theta\ . \end{aligned} \tag{12}$$

E_d and E_u are the deformation potential constants for dilatation and uniaxial strain, respectively, as introduced by Dumke,[24] the polar angle θ is that between the phonon wave vector and the main axis of the energy ellipsoid, $\bar{v}$ is the average sound velocity as defined by Wiley,[25] and ρ is the crystal density. The term $\cos^2\theta$ as a function of the azimuthal angles β,β' and the polar angles α,α' of the wave vectors before and after the scattering process is given by Herring and Vogt[11]:

$$\cos^2\theta=\frac{(\cos\beta'-\cos\beta)^2}{(\cos\beta'-\cos\beta)^2+(m_\perp^*/m_\parallel^*)[\sin^2\beta'+\sin^2\beta-2\sin\beta'\sin\beta\cos(\alpha-\alpha')]}\ . \tag{13}$$

By the selection rules of Lax and Hopfield,[26] the following three scattering processes contribute to the intervalley phonon scattering:

$$\begin{aligned} &\text{LA }\ g\text{ type with } T_1\approx 307\ \mathrm{K}\ ,\\ &\text{LA }\ f\text{ type with } T_2\approx 540\ \mathrm{K}\ ,\\ &\text{TO }\ f\text{ type with } T_3\approx 680\ \mathrm{K}\ , \end{aligned} \tag{14}$$

where T_i is the temperature corresponding to the phonon energy $\hbar\omega_i$ as given by Costato and Reggiani.[16] New selection rules have been given by Lax and Birman[27] and by Streitwolf[28] which take into account only high-energy phonons; however, as discussed by Norton *et al.*,[29] there is experimental evidence that low-energy phonons also contribute to the intervalley scattering, and we therefore have used the selection rules of Lax and Hopfield.[27] We introduce a common coupling constant D_e for all three of these processes. The transition probabilities for intervalley scattering $W_i^{\mathrm{int}}(\vec{k},\vec{k}')$ are then given[7] by

$$W_i^{\mathrm{int}}(\vec{k},\vec{k}')=\frac{\pi Z_i}{\Omega\rho\omega_i}D_e^2\{n(\omega_i)\delta(\epsilon(\vec{k}')-\epsilon(\vec{k})-\hbar\omega_i)+[n(\omega_i)+1]\delta(\epsilon(\vec{k}')-\epsilon(\vec{k})+\hbar\omega_i)\},\ i=1,2,3 \tag{15}$$

where

$$n(\omega_i)=\left[\exp\left[\frac{\hbar\omega_i}{k_B T}\right]-1\right]^{-1} \tag{16}$$

is the occupation number for phonons and Z_i is the number of equivalent valleys into which the electrons can be scattered: $Z_1=1$, $Z_2=Z_3=4$.

2. Distribution function

In order to get the distribution function from the Boltzmann equation, Eq. (7), we use the well-known method by (a) linearizing the Boltzmann equation with respect to the electric field $\vec{E}$ in order to exclude hot electron effects[7] and (b) expanding the distribution function with respect to the magnetic induction $\vec{B}$ and obtain

$$f(\vec{k})=f_0(\epsilon(\vec{k}))-\frac{\partial f_0(\epsilon(\vec{k}))}{\partial\epsilon}\vec{\phi}(\vec{k})\cdot\vec{E}\ , \tag{17}$$

where $f_0(\epsilon(\vec{k}))$ is the Fermi-Dirac distribution function describing the undisturbed states, and the components of the still unknown function $\vec{\phi}(\vec{k})$ are given by

$$\phi_j(\vec{k})=\phi_j^0(\vec{k})+\sum_l \phi_{jl}^0(\vec{k})B_l+\cdots\ ,\quad j,l=1,2,3\ . \tag{18}$$

Inserting Eq. (18) into Eq. (17) and $f(\vec{k})$ into Eqs. (7)–(9), we can solve the Boltzmann equation successively in ascending powers of the magnetic induction $\vec{B}$ as suggested by Fogarassy[30]:

$$\begin{aligned}-\frac{e}{\hbar}[\vec{\nabla}_{\vec{k}}\epsilon(\vec{k})]_j=&\frac{\Omega}{8\pi^3}\sum_{i=1}^{3}\int\left[W_i^{\rm int}(\vec{k},\vec{k}')\phi_j^0(\vec{k})-W_i^{\rm int}(\vec{k}',\vec{k})\phi_j^0(\vec{k}')\frac{\partial f_0(\epsilon(\vec{k}'))}{\partial\epsilon}\Big/\frac{\partial f_0(\epsilon(\vec{k}))}{\partial\epsilon}\right]d\vec{k}'\\ &+\frac{\Omega}{8\pi^3}\int W^{\rm ac}(\vec{k},\vec{k}')\left[\phi_j^0(\vec{k})-\phi_j^0(\vec{k}')\frac{\partial f_0(\epsilon(\vec{k}'))}{\partial\epsilon}\Big/\frac{\partial f_0(\epsilon(\vec{k}))}{\partial\epsilon}\right]d\vec{k}'\ ,\quad j=1,2,3\end{aligned} \tag{19}$$

and

$$\begin{aligned}-\frac{e}{\hbar^2}\Omega_l[\phi_j^0(\vec{k})]=&\frac{\Omega}{8\pi^3}\sum_{i=1}^{3}\int\left[W_i^{\rm int}(\vec{k},\vec{k}')\phi_{jl}^0(\vec{k})-W_i^{\rm int}(\vec{k}',\vec{k})\phi_{jl}^0(\vec{k}')\frac{\partial f_0(\epsilon(\vec{k}'))}{\partial\epsilon}\Big/\frac{\partial f_0(\epsilon(\vec{k}))}{\partial\epsilon}\right]d\vec{k}'\\ &+\frac{\Omega}{8\pi^3}\int W^{\rm ac}(\vec{k},\vec{k}')\left[\phi_{jl}^0(\vec{k})-\phi_{jl}^0(\vec{k}')\frac{\partial f_0(\epsilon(\vec{k}'))}{\partial\epsilon}\Big/\frac{\partial f_0(\epsilon(\vec{k}))}{\partial\epsilon}\right]d\vec{k}',\quad j=1,2,3\end{aligned} \tag{20}$$

where $\vec{\Omega}$ is the operator

$$\vec{\Omega}=\vec{\nabla}_{\vec{k}}\epsilon(\vec{k})\times\vec{\nabla}_{\vec{k}}\ . \tag{21}$$

As shown by Beer,[6] the operator $\vec{\Omega}$ commutes with any function which is a function of energy only.

The integral equations, Eqs. (19) and (20), are solved by expanding $\phi_j^0(\vec{k})$ and $\phi_{jl}^0(\vec{k})$ in spherical harmonics. If the expansion is carried out up to $l=1$ only, the resulting algebraic system of equations reduces to the well-known relaxation-time formalism. The details of the calculation are presented in the Appendix. Insofar as this approximation is justified, this method offers the possibility for calculating the relaxation time not only with all details of the band structure included but also directly from the deformation potential constants. The error introduced by neglecting all terms with $1\geq 2$ of the expansion of $\phi_j^0(\vec{k})$ and $\phi_{jl}^0(\vec{k})$ causes an incorrect influence of the deformation-potential constants. Comparison of the deformation-potential constants, derived by fitting transport coefficients to experimental data, with those obtained from pressure experiments makes it possible for testing the approximations introduced. This comparison is given in Sec. III B.

We obtain the distribution function

$$\phi_j^0(\vec{k})=-\frac{e}{\hbar}[\vec{\nabla}_{\vec{k}}\epsilon(\vec{k})]_j\bar{\tau}_j(\epsilon),\quad \phi_{jl}^0(\vec{k})=\frac{e^2}{\hbar m_j^*}[\vec{\nabla}_{\vec{k}}\epsilon(\vec{k})]_n\bar{\tau}_j(\epsilon)\bar{\tau}_n(\epsilon)\epsilon_{njl}\ , \tag{22}$$

where ϵ_{njl} is the ϵ tensor defined by $\epsilon_{123}=\epsilon_{231}=\epsilon_{312}=1$, $\epsilon_{132}=\epsilon_{321}=\epsilon_{213}=-1$, and all other $\epsilon_{njl}=0$. $\bar{\tau}_j(\epsilon)$ is an energy-dependent function which is given by

$$\frac{1}{\bar{\tau}_j(\epsilon)}=\frac{1}{\tau_1^{\rm int}}+\frac{1}{\tau_2^{\rm int}}+\frac{1}{\tau_3^{\rm int}}+\frac{1}{\tau_j^{\rm ac}}\ ,\quad j=1,2,3\ . \tag{23}$$

$\bar{\tau}_j(\epsilon)$ has the dimension of seconds and is the well-known relaxation time. The terms of Eq. (23) are the following.

(a) Relaxation time of intervalley phonon scattering:

$$\frac{1}{\tau_i^{\mathrm{int}}(\epsilon)}=\frac{Z_i(m_{\parallel}^{*}m_{\perp}^{*2})^{1/2}\sqrt{2}}{\hbar^3\rho 2\pi\omega_i}D_e^2\{n(\omega_i)(\epsilon+\hbar\omega_i)^{1/2}+[n(\omega_i)+1](\epsilon-\hbar\omega_i)^{1/2}\}\ ,\quad i=1,2,3 \tag{24}$$

where the meaning of $i=1,2,3$ is explained by Eq. (14).

(b) Relaxation time of acoustic-phonon scattering:

$$\frac{1}{\tau_{\parallel}^{\mathrm{ac}}(\epsilon)}=\frac{(m_{\parallel}^{*}m_{\perp}^{*2})^{1/2}\sqrt{2}k_BT\sqrt{\epsilon}}{\hbar^4\rho\pi\bar{v}^2}E_1^2\ ,$$

$$\frac{1}{\tau_{\perp}^{\mathrm{ac}}(\epsilon)}=\frac{(m_{\parallel}^{*}m_{\perp}^{*2})^{1/2}\sqrt{2}k_BT\sqrt{\epsilon}}{\hbar^4\rho\pi\bar{v}^2}E_2^2\ , \tag{25}$$

where $j=1,2$ applies to the $\perp$ components and $j=3$ applies to the $\parallel$ component, as given by Eq. (10). The components E_1^2 and E_2^2 depend on the deformation-potential constants E_d and E_u, as introduced in Sec. II A 1, and on numerical constants $\xi_{\parallel}$, $\eta_{\parallel}$, $\xi_{\perp}$, $\eta_{\perp}$ in the following way:

$$E_1^2=E_d^2\left[1+\xi_{\parallel}\frac{E_u}{E_d}+\eta_{\parallel}\frac{E_u^2}{E_d^2}\right]\ ,$$

$$E_2^2=E_d^2\left[1+\xi_{\perp}\frac{E_u}{E_d}+\eta_{\perp}\frac{E_u^2}{E_d^2}\right]\ . \tag{26}$$

The numerical constants are given in the Appendix as

$$\xi_{\parallel}=1.62\ ,$$
$$\eta_{\parallel}=1.32\ ,$$
$$\xi_{\perp}=0.83\ , \tag{27}$$
$$\eta_{\perp}=0.68\ .$$

These values differ by a factor as large as 1.3 from those given by Herring and Vogt,[11] who used a somewhat different approximation. The value of these constants depends on the degree of approximation used in solving the Boltzmann equation. The exact value of these constants has not yet been determined.

B. Valence band

The valence band of Si consists of three atomic p-type bands[31] of which two, the heavy-hole band, denoted by the index $i=1$, and the light-hole band, denoted by the index $i=2$, are degenerate at $\vec{k}=0$. The third band, denoted by the index $i=3$, is separated from the first two bands by the energy Δ, $\Delta=0.044$ eV, due to spin-orbit coupling.[32] In the intrinsic temperature region a considerable fraction of the holes occupy the third band, which therefore has to be taken into account and gives a contribution to the transport coefficients. For the calculation of the transport coefficients, the following system of Boltzmann equations has to be solved:

$$\left[\frac{\partial f^{(i)}}{\partial t}\right]_{\mathrm{field}}+\left[\frac{\partial f^{(i)}}{\partial t}\right]_{\mathrm{coll}}=0,\qquad i=1,2,3\ . \tag{28}$$

In order to overcome mathematical difficulties, we approximate the warped energy surfaces by spheres with effective masses given by Costato *et al.*[32] As pointed out by Wiley,[33] the consequence of this is that the scattering of holes between the split-off ($i=3$) and the other bands ($i=1,2$) is omitted.

1. Transition probabilities

The two relevant scattering mechanisms are the hole—acoustic-phonon scattering and the hole—optical-phonon scattering. We treat both scattering processes by the deformation-potential method introduced by Bardeen and Shockley[13] and Meyer[14] and obtain the following for the transition probabilities.

(a) Acoustic-phonon scattering:

$$W_{ij}^{\mathrm{ac}}(\vec{k},\vec{k}')=\frac{2\pi k_BT}{\hbar\Omega\rho\bar{v}^2}E_0^2G_{ij}(\vec{k},\vec{k}')\delta(\epsilon^{(j)}(\vec{k}')-\epsilon^{(i)}(\vec{k})),\quad i,j=1,2,3\ . \tag{29}$$

(b) Optical-phonon scattering:

$$W_{ij}^{\mathrm{op}}(\vec{\mathrm{k}},\vec{\mathrm{k}}')=\frac{\pi\omega_0}{\Omega\rho\bar{v}^2}E_{\mathrm{NPO}}^2 G_{ij}(\vec{\mathrm{k}},\vec{\mathrm{k}}')\{n(\omega_0)\delta(\epsilon^{(j)}(\vec{\mathrm{k}}')-\epsilon^{(i)}(\vec{\mathrm{k}})-\hbar\omega_0)$$
$$+[n(\omega_0)+1]\delta(\epsilon^{(j)}(\vec{\mathrm{k}}')-\epsilon^{(i)}(\vec{\mathrm{k}})+\hbar\omega_0)\}\ ,\quad i,j=1,2,3\ . \tag{30}$$

The overlap integrals $G_{ij}(\vec{\mathrm{k}},\vec{\mathrm{k}}')$ are taken from Wiley[33]:

$$\begin{aligned}
&G_{11}(\vec{\mathrm{k}},\vec{\mathrm{k}}')=G_{22}(\vec{\mathrm{k}},\vec{\mathrm{k}}')=\tfrac{1}{4}(1+3\cos^2\gamma)\ ,\\
&G_{12}(\vec{\mathrm{k}},\vec{\mathrm{k}}')=G_{21}(\vec{\mathrm{k}},\vec{\mathrm{k}}')=\tfrac{3}{4}\sin^2\gamma\ ,\\
&G_{13}(\vec{\mathrm{k}},\vec{\mathrm{k}}')=G_{31}(\vec{\mathrm{k}},\vec{\mathrm{k}}')\\
&\qquad=G_{32}(\vec{\mathrm{k}},\vec{\mathrm{k}}')=G_{23}(\vec{\mathrm{k}},\vec{\mathrm{k}}')=0\ ,\\
&G_{33}(\vec{\mathrm{k}},\vec{\mathrm{k}}')=1\ ,
\end{aligned} \tag{31}$$

where $i=j$ refers to intraband and $i\neq j$ to interband transitions. The angle γ is that between $\vec{\mathrm{k}}$ and $\vec{\mathrm{k}}'$; ω_0 is the frequency of the optical phonon. The quantities E_0 and E_{NPO} are the deformation-potential constants. Since the pressure dependence of the valence band exhibits a rather complicated behavior, these constants have a mere phenomenological meaning.

2. Distribution function

Since the transition probabilities of acoustic- and optical-phonon scattering are momentum randomizing, the in-scattering term of the Boltzmann equation, Eq. (9), does not contribute to the collision term. As a consequence, originally coupled equations of the light- and heavy-hole band are decoupled, and the Boltzmann equations are solved in the same way as that for the conduction band. We obtain for the distribution functions

$$\begin{aligned}
&\phi_j^{0(i)}(\vec{\mathrm{k}})=\frac{e}{\hbar}[\vec{\nabla}_{\vec{\mathrm{k}}}\epsilon^{(i)}(\vec{\mathrm{k}})]_j\bar{\tau}_i(\epsilon)\ ,\\
&\phi_{jl}^{0(i)}(\vec{\mathrm{k}})=\frac{e^2}{\hbar m_i^*}[\vec{\nabla}_{\vec{\mathrm{k}}}\epsilon^{(i)}(\vec{\mathrm{k}})]_n\bar{\tau}_i^2(\epsilon)\epsilon_{njl}\ ,
\end{aligned} \tag{32}$$

where the index j denotes the spatial component and $i=1,2,3$ the three different bands. We have

$$\frac{1}{\bar{\tau}_i(\epsilon)}=\frac{1}{\tau_i^{\mathrm{ac}}(\epsilon)}+\frac{1}{\tau_i^{\mathrm{op}}(\epsilon)}\ , \tag{33}$$

where the acoustic- and optical-phonon relaxation times are given by

$$\frac{1}{\tau_i^{\mathrm{ac}}(\epsilon)}=(\bar{m}^{(i)})^{3/2}\frac{\sqrt{2}k_BT\sqrt{\epsilon}}{\hbar^4\rho\pi\bar{v}^2}E_0^2\ , \tag{34}$$

$$\frac{1}{\tau_i^{\mathrm{op}}(\epsilon)}=(\bar{m}^{(i)})^{3/2}\frac{\sqrt{2}\omega_0}{\hbar^3\rho 2\pi\bar{v}^2}E_{\mathrm{NPO}}^2$$
$$\times\{n(\omega_0)(\epsilon+\hbar\omega_0)^{1/2}$$
$$+[n(\omega_0)+1](\epsilon-\hbar\omega_0)^{1/2}\}\ , \tag{35}$$

with

$$\begin{aligned}
&(\bar{m}^{(1)})^{3/2}=(\bar{m}^{(2)})^{3/2}=\tfrac{1}{2}(m_1^{*3/2}+m_2^{*3/2})\ ,\\
&(\bar{m}^{(3)})^{3/2}=m_3^{*3/2}\ .
\end{aligned} \tag{36}$$

In our calculation, the relaxation times for light and heavy holes are identical. Brown and Bray[34] assume that light and heavy holes are predominantly scattered into the heavy-hole band where the density of states is much higher than that in the light-hole band, and they assume that scattering into the light-hole band may be neglected. They conclude that the relaxation times for light and heavy holes must be identical. Our calculations show that their conclusion is, in fact, correct even if scattering into the light-hole band is allowed.

C. Transport coefficients

In n-type material it is permissible to neglect the influence of the valence band up to the intrinsic temperature region, since the mobility of electrons is much higher than that of holes. From the theory of anisotropic scattering in crystals with many-valley structures as formulated by Herring and Vogt[11] and Ohta and Sakata,[35] two basic temperature-dependent transport coefficients are obtained.

(a) The Hall factor r_n:

$$r_n=\frac{\dfrac{1}{3}\dfrac{\langle\bar{\tau}_\perp\bar{\tau}_\perp\rangle}{m_\perp^{*2}}+\dfrac{2}{3}\dfrac{\langle\bar{\tau}_\perp\bar{\tau}_\parallel\rangle}{m_\perp^* m_\parallel^*}}{\left[\dfrac{1}{3}\dfrac{\langle\bar{\tau}_\parallel\rangle}{m_\parallel^*}+\dfrac{2}{3}\dfrac{\langle\bar{\tau}_\perp\rangle}{m_\perp^*}\right]^2}\ . \tag{37}$$

(b) The drift mobility $\mu_d^{(n)}$:

$$\mu_d^{(n)}=e\left[\frac{1}{3}\frac{\langle\bar{\tau}_{\parallel}\rangle}{m_{\parallel}^{*}}+\frac{2}{3}\frac{\langle\bar{\tau}_{\perp}\rangle}{m_{\perp}^{*}}\right] . \tag{38}$$

If the holes in the valence band are neglected, the Hall coefficient R_H is

$$R_H=-\frac{r_n}{en} , \tag{39}$$

and the conductivity σ_0 is

$$\sigma_0=en\mu_d^{(n)} . \tag{40}$$

A quantity often determined experimentally is the Hall mobility $\mu_H^{(n)}$, defined as

$$\mu_H^{(n)}=r_n\mu_d^{(n)}=|R_H|\,|\sigma_0| , \tag{41}$$

which is not explicitly dependent on the carrier density and, as discussed in Sec. III, is useful only in a rather limited temperature region.

The angular brackets in Eqs. (37) and (38) represent an appropriate averaging integral defined[6] as

$$\langle\bar{\tau}\rangle\equiv\frac{\int_0^{\infty}\bar{\tau}(\epsilon)\frac{\partial f_0}{\partial\epsilon}\epsilon^{3/2}d\epsilon}{\int_0^{\infty}\frac{\partial f_0}{\partial\epsilon}\epsilon^{3/2}d\epsilon} . \tag{42}$$

In p-type material the contribution of the electrons to transport coefficients is not negligible over a wide temperature region. Therefore, we write the transport coefficients as a function of both carrier types. According to Eq. (4), the Hall coefficient R_H and the conductivity σ_0 have the following form:

$$R_H=\frac{\sigma_{123}^{0(n)}+\sigma_{123}^{0(p)}}{(\sigma_{11}^{0(n)}+\sigma_{11}^{0(p)})^2} , \tag{43}$$

$$\sigma_0=\sigma_{11}^{0(n)}+\sigma_{11}^{0(p)} , \tag{44}$$

where the indices (n) and (p) refer to electrons and holes, respectively. For the valence band, the components of the conductivity tensors are the sums of the contributions of the three subbands. Inserting Eqs. (32) and (17) into Eq. (6) we get, according to Eq. (3),

$$\begin{aligned}\sigma_{11}^{0(p)}&=\frac{p_1e^2\langle\bar{\tau}_1\rangle}{m_1^{*}}+\frac{p_2e^2\langle\bar{\tau}_2\rangle}{m_2^{*}}+\frac{p_3e^2\langle\bar{\tau}_3\rangle}{m_3^{*}} ,\\ \sigma_{123}^{0(p)}&=\frac{p_1e^3\langle\bar{\tau}_1^2\rangle}{m_1^{*2}}+\frac{p_2e^3\langle\bar{\tau}_2^2\rangle}{m_2^{*2}}+\frac{p_3e^3\langle\bar{\tau}_3^2\rangle}{m_3^{*2}} .\end{aligned} \tag{45}$$

From these, we obtain the following expressions for the Hall coefficient R_H and conductivity σ_0, respectively,

$$R_H=\frac{-ne^3\left[\frac{1}{3}\frac{\langle\bar{\tau}_{\perp}\bar{\tau}_{\perp}\rangle}{m_{\perp}^{*2}}+\frac{2}{3}\frac{\langle\bar{\tau}_{\perp}\bar{\tau}_{\parallel}\rangle}{m_{\perp}^{*}m_{\parallel}^{*}}\right]+pe^3\left[\gamma_1\frac{\langle\bar{\tau}_1^2\rangle}{m_1^{*2}}+\gamma_2\frac{\langle\bar{\tau}_2^2\rangle}{m_2^{*2}}+\gamma_3\frac{\langle\bar{\tau}_3^2\rangle}{m_3^{*2}}\right]}{\left[ne^2\left[\frac{1}{3}\frac{\langle\bar{\tau}_{\parallel}\rangle}{m_{\parallel}^{*}}+\frac{2}{3}\frac{\langle\bar{\tau}_{\perp}\rangle}{m_{\perp}^{*}}\right]+pe^2\left[\gamma_1\frac{\langle\bar{\tau}_1\rangle}{m_1^{*}}+\gamma_2\frac{\langle\bar{\tau}_2\rangle}{m_2^{*}}+\gamma_3\frac{\langle\bar{\tau}_3\rangle}{m_3^{*}}\right]\right]^2} , \tag{46}$$

$$\sigma_0=ne^2\left[\frac{1}{3}\frac{\langle\bar{\tau}_{\parallel}\rangle}{m_{\parallel}^{*}}+\frac{2}{3}\frac{\langle\bar{\tau}_{\perp}\rangle}{m_{\perp}^{*}}\right]+pe^2\left[\gamma_1\frac{\langle\bar{\tau}_1\rangle}{m_1^{*}}+\gamma_2\frac{\langle\bar{\tau}_2\rangle}{m_2^{*}}+\gamma_3\frac{\langle\bar{\tau}_3\rangle}{m_3^{*}}\right] , \tag{47}$$

$$\sigma_0=e(n\mu_d^{(n)}+p\mu_d^{(p)}) , \tag{48}$$

where the γ_i, $i=1,2,3$, are fractional carrier densities defined by

$$\begin{aligned}\gamma_1&=\frac{p_1}{p}=\left[1+\left[\frac{m_2^{*}}{m_1^{*}}\right]^{3/2}+\left[\frac{m_3^{*}}{m_1^{*}}\right]^{3/2}e^{-T_0/T}\right]^{-1} ,\\ \gamma_2&=\frac{p_2}{p}=\left[1+\left[\frac{m_1^{*}}{m_2^{*}}\right]^{3/2}+\left[\frac{m_3^{*}}{m_2^{*}}\right]^{3/2}e^{-T_0/T}\right]^{-1} ,\\ \gamma_3&=\frac{p_3}{p}=\left[1+\left[\frac{m_1^{*}}{m_3^{*}}\right]^{3/2}e^{T_0/T}+\left[\frac{m_2^{*}}{m_3^{*}}\right]^{3/2}e^{T_0/T}\right]^{-1} ,\end{aligned} \tag{49}$$

with $p=p_1+p_2+p_3$ and $\gamma_1+\gamma_2\,\gamma_3=1$. $T_0=510$ K is the temperature connected with the spin-orbit splitting of the valence band $\Delta=44$ meV. These fractional densities are temperature dependent due to the split-off valence band.

By rearrangement of Eq. (46) and by comparison with the formula for the Hall coefficient, Eq. (1), we obtain the Hall factor r_p:

$$r_p=\frac{\gamma_1\frac{\langle\bar{\tau}_1^2\rangle}{m_1^{*2}}+\gamma_2\frac{\langle\bar{\tau}_2^2\rangle}{m_2^{*2}}+\gamma_3\frac{\langle\bar{\tau}_3^2\rangle}{m_3^{*2}}}{\left[\gamma_1\frac{\langle\bar{\tau}_1\rangle}{m_1^{*}}+\gamma_2\frac{\langle\bar{\tau}_2\rangle}{m_2^{*}}+\gamma_3\frac{\langle\bar{\tau}_3\rangle}{m_3^{*}}\right]^2}\ . \tag{50}$$

By comparing Eq. (47) with Eq. (48), we obtain the drift mobility of the holes $\mu_d^{(p)}$

$$\mu_d^{(p)}=e\left[\gamma_1\frac{\langle\bar{\tau}_1\rangle}{m_1^{*}}+\gamma_2\frac{\langle\bar{\tau}_2\rangle}{m_2^{*}}+\gamma_3\frac{\langle\bar{\tau}_3\rangle}{m_3^{*}}\right]\ . \tag{51}$$

The Hall mobility of holes $\mu_H^{(p)}$ can be expressed in a form similar to Eq. (41) and is given by

$$\mu_H^{(p)}=\mu_d^{(p)}r_p\ . \tag{52}$$

The temperature dependence of the Hall factors is basically due to the temperature dependence of the scattering mechanisms. In the valence band, there is an additional contribution due to the temperature dependence of the fractional hole densities in the three subbands. A third contribution arises if different temperature dependences of the effective masses are assumed, but this effect is not considered here.

III. APPLICATION OF THE THEORY TO EXPERIMENTAL RESULTS

A. Experimental

The Hall coefficient R_H and the conductivity σ_0 were determined experimentally in the temperature range 90–450 K by using a conventional Hall-effect apparatus. Experimentally, the Hall coefficient R_H is given by Kubo and Nagamiya[36] as

$$R_H=\frac{U_y d}{i_x B_z}\ , \tag{53}$$

where U_y is the Hall voltage, i_x the current, B_z the magnetic induction, and d the sample thickness.

In order to measure the temperature variation of R_H and σ_0, a constant nitrogen-gas stream in combination with a special proportional integrating differentiating regulator was used.[37] This arrangement allows us to vary the temperature of the sample with an uncertainty smaller than 5 K. The magnetic field used was $B_z=1.3$ T, with an inhomogenity of less than 10^{-4} as determined by proton resonance.

The silicon samples were cut from single crystals, of dislocation-free Wacker material in the direction of the (111) plane, and had dimensions $11\times2.5\times0.8$ mm^3. Electric contacts were applied by discharge bonding[38] with the gold wires doped in accordance with the crystal doping. The current i_x, supplied by a constant current source, was chosen such that the electric power remains smaller than 1 μW.

Before each measurement, the zero-field Hall voltage was compensated and measurements were taken for both directions of both the current and the magnetic induction. The uncertainty of the Hall coefficient was determined by the uncertainty in the electrical measurement (about 1%) and the uncertainty in the sample thickness (about 3%). The uncertainty in the conductivity was about 5%.

B. Comparison of experimental results with theory

In order to obtain carrier concentrations from the Hall coefficient, Eq. (1), the temperature dependence of the Hall factors and the mobilities must be known. By using Eqs. (37) and (50) for the Hall factors and Eqs. (38) and (51) for the drift mobilities, it is only necessary to know the deformation-potential constants.

For n-type material, the best way to obtain the unknown parameters is to use the Hall mobility, which is the product $(R_H\sigma_0)_{\text{expt}}$ of the experimental Hall coefficient and experimental conductivity. Up to the intrinsic temperature region, the Hall mobility $\mu_H^{(n)}$ of electrons is independent of the carrier concentration. Fitting the theoretical curve $\mu_H^{(n)}$ [Eq. (41) in combination with Eqs. (37) and (38)] to the experimental values of Fig. 1 and using the material constants $m_\perp^*=0.19m_0$, $m_\parallel^*=0.91m_0$, $\rho=2.33\times10^3$ kg/m^3, and $\bar{v}=9.04\times10^3$ m/s of Si as given by Costato and Reggiani,[16] we obtain the following deformation potential constants:

$$\begin{aligned} E_d&=-9.41\text{ eV}\ ,\\ E_u&=+12.97\text{ eV}\ ,\\ D_e&=3.54\times10^8\text{ eV/cm}\ . \end{aligned} \tag{54}$$

The so called K parameter

$$K=\frac{\tau_\perp^{\text{ac}}(\epsilon)}{\tau_\parallel^{\text{ac}}(\epsilon)} \tag{55}$$

is the only parameter which cannot be fitted by this method. We therefore take $K=1.1$ as obtained by Stradling and Zhukov[39] from cyclotron-resonance experiments. It may be noted that the deformation-potential constants E_d and E_u are rather sensitive to

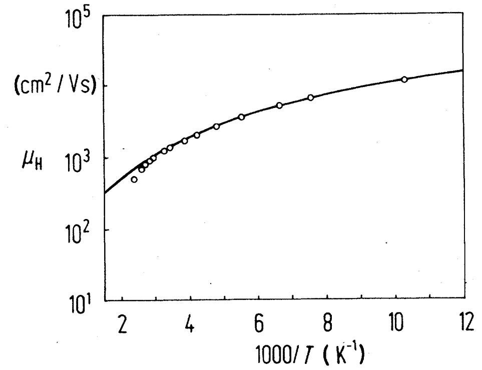

FIG. 1. Hall mobility of an n-type sample as a function of temperature. Circles: experimental values. Solid line: best-fit curve according to Eq. (41).

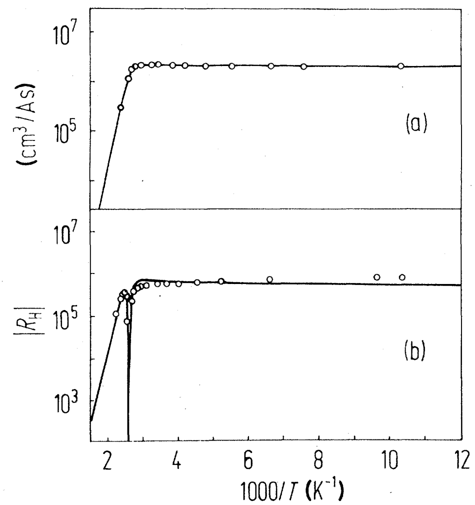

FIG. 2. Hall coefficient as a function of temperature. (a) n-type sample; (b) p-type sample. Circles: experimental values. Solid line: best-fit curve according to Eqs. (39) and (46).

a slight variation of the K parameter. However, the theoretical Hall mobility $\mu_H^{(n)}$ is rather insensitive to a variation of K. Deformation-potential constants $E_d = -6.0$ eV and $E_u = 9.0$ eV obtained by Murase *et al.*[15] are 30% smaller than our values. Our coupling constant D_e, which has been introduced for all three processes of intervalley phonon scattering, Eq. (14), agrees well with the result of Costato and Reggiani,[16] who used two different coupling constants $D_{e,f} = 3 \times 10^8$ eV/cm and $D_{e,g} = 4.5 \times 10^8$ eV/cm.

For the valence band, the product $(R_H\sigma_0)$ has no physical meaning except in a rather limited temperature range. Therefore the procedure used for the conduction band is not applicable here. The experimental Hall coefficient $(R_H)_{\text{expt}}$ and experimental conductivity $(\sigma_0)_{\text{expt}}$ must be fitted independently under the condition that the same set of deformation-potential constants be used for both quantities. In performing the fitting, we use Eq. (46) for R_H and Eq. (47) for σ_0. For the deformation-potential constants of the conduction band we take those given in Eq. (54). The temperature-dependent carrier concentrations in Eq. (46) for the Hall coefficient and Eq. (47) for the conductivity have been expressed by the density of negatively charged acceptors N_A^- and n_i^2 by use of the following equations for p-type crystals:

$$p = \tfrac{1}{2}N_A^- + [(\tfrac{1}{2}N_A^-)^2 + n_i^2]^{1/2} \,,$$

$$n = -\tfrac{1}{2}N_A^- + [(\tfrac{1}{2}N_A^-)^2 + n_i^2]^{1/2} \,. \tag{56}$$

The effect of deionization of the acceptors is negligible in the temperature region considered and we can safely assume $N_A^- = N_A$, where N_A is the density of acceptors. For the intrinsic carrier density we use the equation

$$n_i^2 = 1.5 \times 10^{33} T^3 \exp(-14028/T) \,, \tag{57}$$

as given by Wolf,[10] where n is expressed in units of cm^{-6}, and T is the temperature in units of K. The equations are applicable for crystals with low concentrations of shallow impurities and for temperatures high enough that all acceptors are ionized.

Fitting the theoretical R_H, Eq. (46), to the experimental values [Fig. 2(b)] and simultaneously the theoretical σ_0, Eq. (47), to the experimental values [Fig. 3(b)], we obtain the deformation-potential constant

$$E_0 = 18.42 \text{ eV} \tag{58}$$

and the optical "strength" parameter

$$\eta^2 = \left[\frac{E_{\text{NPO}}}{E_0} \right]^2 = 2.20 \,, \tag{59}$$

where the material constants have been taken from Costato *et al.*[32] and the best doping concentration to be used is $N_A^- = 1.66 \times 10^{13}$ cm^{-3}. Wiley and DiDomenico[17] determined the deformation potential constant from conductivity measurements to be

$$E_0 = 7.9 \text{ eV} \,.$$

This result was obtained by fitting the theoretical drift mobility to the experimental Hall mobility and assuming $r_p = 1$. In addition, they did not include the exact form of the overlap function $G_{ij}(\vec{k},\vec{k}')$.

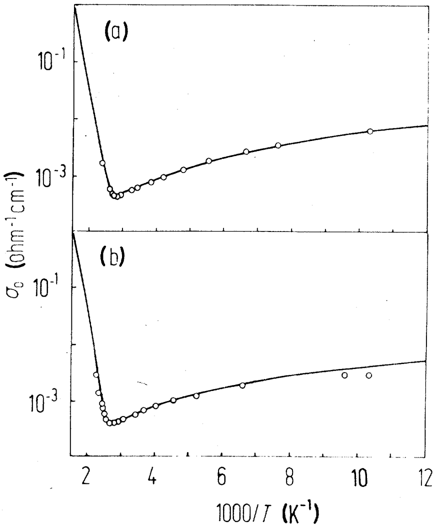

FIG. 3. Conductivity as a function of temperature. (a) n-type sample; (b) p-type sample. Circles: experimental values. Solid line: best-fit curve according to Eqs. (40) and (47).

For n-type crystals, instead of Eq. (56), we use the corresponding equations and obtain the Hall coefficient R_H from Eq. (39) and the conductivity σ_0 from Eq. (40). The result is shown in Figs. 2(a) and 3(a). The best fit it obtained with a donor concentration of $N_D^+ = 3.27 \times 10^{12}$ cm^{-3}. The Hall factors r_n and r_p are calculated from Eqs. (37) and Eq. (50) by using the deformation-potential constants, Eq. (54), for the conduction band and Eqs. (58) and (59) for the valence band. The results are shown in Fig. 4. From this figure it is seen that in the temperature range under discussion, r_n varies between 1.0 and 1.2 and r_p between 1.5 and 2.0. The temperature dependence of the Hall factors is due to intervalley and optical-phonon scattering. The much stronger variation of r_p compared to r_n is caused by the temperature variation of the fractional densities in the three subbands. The dependence of r_p on the splitting of the separated valence band and on the optical phonons expressed by the optical strength parameter η^2, as defined in Eq. (59), is shown in Fig. 5. Without optical-phonon scattering, $\eta^2 = 0$, the Hall factor r_p is constant for $\Delta = 0$ eV. For a large split off energy, i.e., $\Delta = 1$ eV, there is only a negligible dependence on temperature. For an intermediate energy, $\Delta = 0.03$ eV, even without optical-phonon scattering, $\eta^2 = 0$, the Hall factor depends strongly on temperature. For $\eta^2 > 0$, there is a temperature dependence for all split-off energies. In the calculation of r_p for silicon (Fig. 4) parameters $\Delta = 0.044$ eV and $\eta^2 = 2.20$ have been used, which correspond approximately to the third curve of the set $\Delta = 0.03$ eV of Fig. 5.

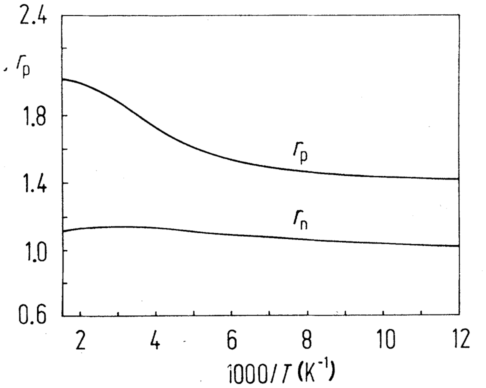

FIG. 4. Hall factors as a function of temperature for the conduction and valence bands.

It is well known that in the case of only one spherical energy band and only acoustic-phonon scattering, the Hall factor is constant and the Hall mobility and drift mobility follow a $T^{-\beta}$ law with $\beta = 1.5$. If one includes for the valence band the temperature variation of the fractional densities in the three subbands, the temperature dependence of the Hall factor becomes larger (as discussed above) and at the same time the temperature dependence of the mobilities becomes smaller, $\beta < 1.5$.

For comparison with experimental results the drift mobilities of electrons and holes calculated with Eqs. (38) and (51) are approximated by an $\alpha T^{-\beta}$ law:

$$\mu_d^{(n)} = 9.40 \times 10^7 T^{-1.97}, \qquad \mu_d^{(p)} = 6.59 \times 10^6 T^{-1.80}, \tag{60}$$

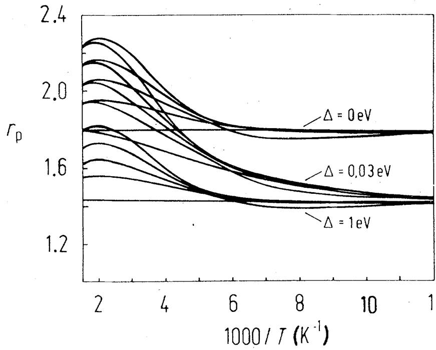

FIG. 5. Temperature dependence of the Hall factor r_p for different values of the optical strength parameter η^2 and the energy Δ of the split-off valence band. For each value of the energy Δ there is given a set of five values η^2. Going upwards, these are $\eta^2 = 0,1,2,4,10$.

with μ in units of $\mathrm{cm}^2/\mathrm{V\,s}$. In the temperature region $160 < T < 400$ K the following laws are given by Ludwig and Watters[40]:

$$\mu_d^{(n)} = 2.1 \times 10^9 T^{-2.5} ,$$
$$\mu_d^{(p)} = 2.3 \times 10^9 T^{-2.7} , \tag{61}$$

again in $\mathrm{cm}^2/\mathrm{V\,s}$. The temperature dependence of these experimental mobilities is much stronger than that of our calculated mobilities. However, comparison of our calculated curves with the experimental points in Figs. 2 and 3 shows that our formulas do fit our experimental results rather well.

This general agreement does not hold for the Hall coefficient of the p-type sample [Fig. 2(b)]. Here there is a serious discrepancy; in particular, in the extrinsic temperature region, the slope of the experimental points is opposite in sign to that of the theoretical curve. In crystals with small concentrations of shallow impurities, the carrier concentration in the extrinsic temperature region can safely be assumed to be a constant.

The negative slope of the experimental Hall coefficient results, therefore, from a negative slope of the experimental Hall factor r_p. This negative slope is not only a result of our experiments, but has also been observed by Long.[41] From the experiments of Long it is seen further that the slope is not due to a rather high magnetic induction, since the experimental points are identical for a magnetic induction of 0.3 and 1.3 T. The contradiction of the slope of the theoretical r_p values (Fig. 4) with experimental results cannot be explained in the frame of our model and needs further investigation.

IV. STRUCTURE OF THE HALL FORMULA

Once the ratio of mobilities b and the Hall factors r_n and r_p are known, the carrier concentrations n and p can be obtained from the experimentally determined Hall coefficient R_H by solving Eq. (1) and using the condition $np = n_i^2$. We define the dimensionless quantities

$$x = \frac{p}{p_0} ,$$
$$\alpha = \frac{r_n}{r_p} b , \tag{62}$$
$$r = \frac{eR_H}{r_p} p_0 = \frac{eR_H \sqrt{b}\, n_i}{r_p} ,$$

where $p_0 = \sqrt{b}\, n_i$ is a normalization factor for the hole concentration. We obtain from Eq. (1) an equation of fourth order in x:

$$f(x) = x^4 - \frac{1}{r} x^3 + 2x^2 + \frac{\alpha}{r} x + 1 = 0 . \tag{63}$$

Only real positive solutions of this equation have a physical meaning. Since for n-type material the hole concentration can be neglected even up to the intrinsic region, we consider in the following p-type material only.

From a theorem of Budan-Fourier[42] it follows[22] that the number z of positive real roots of Eq. (63) is $z = 0$, 1, or 2. The case of a double root or $z = 1$ can be found from Eq. (63) by solving

$$\frac{dr(x)}{dx} = 0 \quad \text{with } r(x) = \frac{x(x^2-\alpha)}{(x^2+1)^2} . \tag{64}$$

Inserting the two solutions

$$x_{1,2}^2 = \tfrac{3}{2}(\alpha+1) \pm \tfrac{3}{2}(\alpha^2 + \tfrac{14}{9}\alpha + 1)^{1/2} \tag{65}$$

into $r(x)$, Eq (64), we get $r(x_{1,2})$ or r as a function of α for which we have $z = 1$. This is shown in the root diagram (Fig. 6) which shows the different regions belonging to $z = 0$ and 2 for all relevant pairs (α, r). On the dividing line between these regions, the pairs (α, r) lead to a double root ($z = 1$). Evidently, the root diagram expresses the condition on α and r for obtaining physically meaningful solutions of Eq. (63). For the case of two different roots, $z = 2$, the corresponding two different carrier

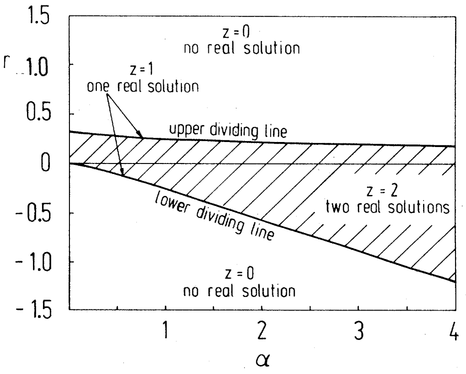

FIG. 6. Root diagram. Dependence of the number of real positive roots z of Eq. (63) on the pairs (α, r) as defined by Eq. (62).

concentrations give rise to the same Hall coefficient.

In order to understand this somewhat surprising result, the Hall coefficients as a function of temperature for different doping concentrations are shown in Fig. 7. With respect to a special doping concentration N_A^0, the curves with concentrations $N_A < N_A^0$ cross the curve with N_A^0 on the right-hand side of the encircled area. The curves with concentrations $N_A > N_A^0$ cross the curve with N_A^0 at the left-hand side of this encircled area. In approaching the curve N_A^0 from lower and higher concentrations, the crossing points of the lower and higher concentrations coincide at one unique point at the temperature $T = T_0$. At this point, only the concentration N_A^0 results in the Hall coefficient $R_H(T_0)$. This means that at each point in the (R_H, $1/T$) diagram, there exist two different solutions corresponding to two carrier concentrations, except for certain points which form a continuous line for which there exists only one solution. The line for only one solution in Fig. 7 (which is not shown explicitly) corresponds to the upper dividing line, $z = 1$, in the root diagram (Fig. 6). A similar line for negative R_H values corresponds to the lower dividing line, $z = 1$, in the root diagram. The total (R_H, $1/T$) plane, except the two lines for one solution, Fig. 6, is mapped into the area $z = 2$ between the two dividing lines of the root diagram. For any doping concentration there exist necessarily two temperatures, where only one carrier concentration is a solution of the Hall formula. At these temperatures the corresponding (α,r) points necessarily lie on the upper and lower dividing line, respectively. This implies an additional condition between α and r for the temperature points with only one solution of the Hall formula.

The question is as follows: What happens if one tries to solve Eq. (1) for an experimentally determined R_H and does not have available the correct material parameters b, r_n, and r_p? The answer is given by Fig. 8(a): It is not possible in this case to obtain a continuous carrier concentration as a function of temperature. This difficulty has been recognized before as shown in Fig. 9, which is taken from Neubert and Schlief.[4] In this case the authors have tried to evaluate the experimental curve for the Hall coefficient [Fig. 9(a)] by using three different sets of transport parameters: (A) $r_n = r_p = \frac{3}{8}\pi$, (B) r_n and r_p as given by Messier and Flores,[5] (C) by using a heuristic set of r_n and r_p, which was chosen such that the carrier concentration becomes continuous in the intermediate temperature region. However, no theoretical explanation of the Hall factors r_n and r_p obtained in this way was attempted.

Comparison of Fig. 8(a) with Fig. 9(b) makes it clear that the evaluation of carrier concentrations as given in Fig. 9(b) does in fact agree with the predictions of the theoretical solutions of the Hall formula for the case in which the transport parameters are not correctly known. The case for which the transport parameters are assumed to be correctly known is shown in Fig. 8(b). This figure was obtained by calculating the Hall coefficient for agiven carrier concentration with a postulated set of transport parameters and then recalculating the carrier concentrations from this artificial Hall coefficient. In principle, a rule for selecting the correct solution for the carrier concentration, can be deduced from Fig. 7. For practical purposes, such a rule is illustrated by Fig. 8(b): Starting from low temperatures, choose the higher solution, after the first crossing point

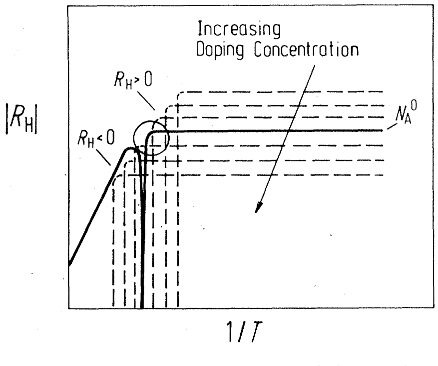

FIG. 7. Temperature dependence of the Hall coefficient for p-type silicon with different doping concentrations (schematic drawing). For the concentrations indicated by dotted lines, R_H is shown only in that temperature interval, in which $R_H > 0$.

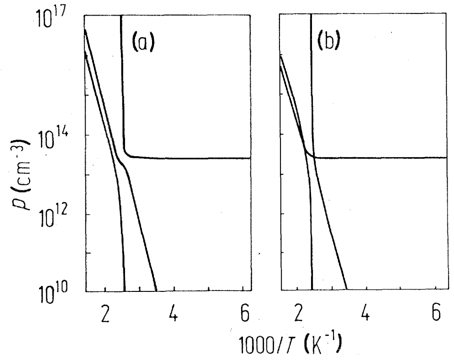

FIG. 8. Solution of the Hall formula by utilizing (a) incorrect transport parameters, and (b) correct transport parameters.

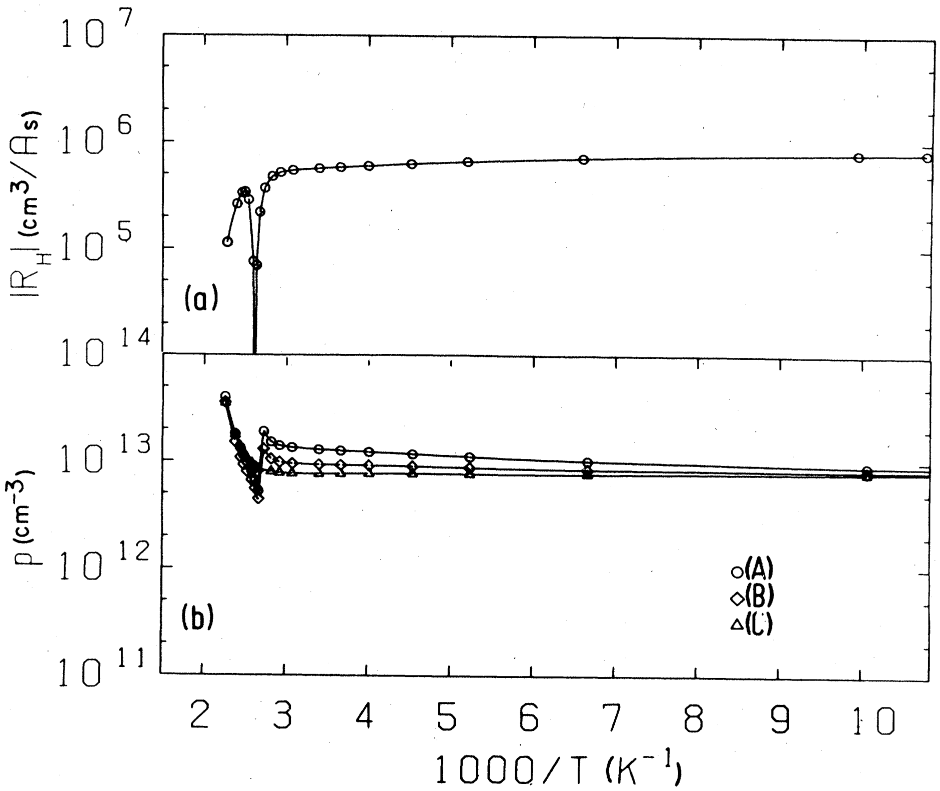

FIG. 9. (a) Hall coefficient of a lightly doped p-type silicon sample as a function of temperature. Circles: experimental points. Solid line: interpolating curve. (b) Calculated carrier concentrations as a function of temperature with various transport parameters. (A) $r_n = r_p = \frac{3}{8}\pi$. (B) r_n and r_p as given by Messier and Flores (Ref. 5). (C) r_n and r_p as given by Neubert and Schlief (Ref. 4).

choose the lower solution, after the point $R_H = 0$, where there is a singularity in the solutions, choose the higher solution, and finally, after the second crossing point, choose the lower solution.

Even though this rule is not very sophisticated, in practice it must be applied in order to obtain the carrier concentration from the Hall coefficient for a given crystal. As seen clearly from Fig. 8, there is the risk that one may choose the wrong solution in evaluating Hall measurements. This holds especially for the case of materials with deep traps, such as dislocations, where there does not exist an extrinsic temperature region with a constant carrier density.

V. DISCUSSION

In this paper we have shown that the evaluation of carrier densities from Hall-effect measurements depends very sensitively on the Hall factors r_n and r_p, since there is a discontinuity in the temperature dependence of the carrier densities if the Hall factors are not correct. It is to be noted that a specific physical model, on which the calculation of r_n and r_p is based, should at the same time correctly predict not only the Hall coefficient R_H, but also the conductivity σ_0. In the literature, it is rather common to report experimental results not for R_H and σ_0 independently but for their product, the Hall mobility $\mu_H = \sigma_0 R_H$. Correspondingly, models are constructed to explain only this quantity. Consequently, these models have not been general enough to calculate the accurate Hall factors necessary for deducing carrier concentrations from the Hall coefficient. In this paper we have considered explicitly besides the Hall mobility also the Hall factors.

For the conduction band, the assumption of six energy ellipsoids with acoustic- and intervalley phonon scattering as the only scattering processes can be used to describe the Hall mobility with sufficient accuracy. However, there are more then one set of selection rules of intervalley phonon scattering and coupling constants which lead to the same temperature dependence for the Hall mobility. It has been shown by Ohta and Sakata[35] that each of these sets leads to a different temperature dependence of r_n.

We have taken the selection rules of Lax and Hopfield[26] and have obtained with our coupling constant a Hall factor which is in agreement with experiment. However, it should be noted that the Hall factor is rather insensitive to selection rules and coupling constants. Therefore it is possible that some other set of selection rules and coupling constants may also give agreement with experimental Hall-effect measurements and that our particular choice is not unique.

With respect to the valence band, it has been shown in this paper that the model of acoustic- and optical-phonon scattering with the assumption of spherical energy surfaces is appropriate for explaining the temperature-dependent Hall mobility of holes. But within the framework of this model, it is not readily possible to explain the experimental negative slope of the temperature dependence of the Hall factor r_p.

In the search for possible refinements of our model, some additional factors reported in the literature may be considered. By taking into account the warping of the energy surfaces as has been done by Lax and Mavroides,[19] one can obtain a decrease of r_p by a constant factor independent of temperature. The inclusion of the temperature dependence of effective masses as given by Costato *et al.*,[32] does not help to resolve this question, since this leads to an actual increase of the positive slope of the theoretical Hall factor r_p. Roizes and Schuttler[43] have also taken into account, in their calculations of Hall factors, the cubic symmetry of hole—acoustic-phonon scattering. This change from spherical to cubic symmetry results (from their numerical evaluation) again in a temperature-independent contribution. There is one effect, which has been called "shape evolution" by Allgaier,[44] which might resolve the discrepancy between theory and experiment. Shape evolution in metals describes the manner in which a Fermi surface changes shape with the Fermi energy; a similar effect may be important for the valence band of silicon. The inclusion of shape evolution requires that one must solve the system of coupled Boltzmann equations not for spherical but for cubic symmetry (of the bands and of the scattering processes). This has been done so far only for the valence band of Ge by Lawaetz.[45] It seems of interest to perform such calculations also for Si in order to see if shape evolution is sufficiently strong to change the slope of the temperature dependence of r_p.

Finally, it has been pointed out in this paper that even if r_n and r_p are known exactly, one should be very careful in selecting the right solution of the Hall formula. This point becomes especially important in those cases where there exists no temperature range over which the carrier density is constant.

ACKNOWLEDGMENT

We thank H. Künzel for various technical assistance.

APPENDIX

In order to solve Eqs. (19) and (20) we use the following new coordinates in $\vec{k}$ space for each of the six ellipsoids (m_0= electron mass)

$$
\begin{aligned}
p_1 &= \left[\frac{m_0}{m_1^*} \right]^{1/2} k_1 , \\
p_2 &= \left[\frac{m_0}{m_2^*} \right]^{1/2} k_2 , \\
p_3 &= \left[\frac{m_0}{m_3^*} \right]^{1/2} k_3 ,
\end{aligned}
\tag{A1}
$$

so that the constant-energy surfaces, Eq. (10), are given by

$$
\epsilon(\vec{p}) = \frac{\hbar^2 \vec{p}^{\,2}}{2m_0}
\tag{A2}
$$

With these new coordinates the operator $\vec{\Omega}$, Eq. (21), now reads

$$
\Omega_l = \frac{\hbar^2 (m_l^*)^{1/2}}{m_\perp^* (m_\parallel^*)^{1/2}} (\vec{p} \times \vec{\nabla}_{\vec{p}})_l ,
\tag{A3}
$$

and we have terms in spherical coordinates p,β,α of the form:

$$
-\frac{e}{\hbar} [\vec{\nabla}_{\vec{k}} \epsilon(\vec{k})]_j = g_j(\epsilon) h_j(\beta,\alpha) , \quad j=1,2,3
\tag{A4}
$$

with

$$
g_j(\epsilon) = -e \left[\frac{8\pi\epsilon}{3m_j^*} \right]^{1/2} .
\tag{A5}
$$

The terms $h_j(\beta,\alpha)$ are real spherical harmonics. For $j=1,2,3$, we have

$$\begin{aligned} h_1 &= \left[\frac{3}{4\pi}\right]^{1/2}\frac{p_1}{p} = \left[\frac{3}{4\pi}\right]^{1/2}\sin\beta\cos\alpha\ , \\ h_2 &= \left[\frac{3}{4\pi}\right]^{1/2}\frac{p_2}{p} = \left[\frac{3}{4\pi}\right]^{1/2}\sin\beta\sin\alpha\ , \\ h_3 &= \left[\frac{3}{4\pi}\right]^{1/2}\frac{p_3}{p} = \left[\frac{3}{4\pi}\right]^{1/2}\cos\beta\ . \end{aligned} \tag{A6}$$

In terms of spherical coordinates $d\vec{k}$ now reads

$$d\vec{k} = \frac{(2m_\perp^{*2}m_\parallel^*)^{1/2}}{\hbar^3}\sqrt{\epsilon}\,d\epsilon\,d\Omega\ , \tag{A7}$$

and $d\Omega = \sin\beta d\beta d\alpha$.

We can expand the distribution function in terms of the real spherical harmonics $h_n(\beta,\alpha)$

$$\begin{aligned} \phi_j^0(\vec{p}) &= \sum_{n=1}^{\infty}\varphi_{jn}(\epsilon)h_n(\beta,\alpha)\ , \\ \phi_{jl}^0(\vec{p}) &= \sum_{n=1}^{\infty}\varphi_{jln}(\epsilon)h_n(\beta,\alpha)\ . \end{aligned} \tag{A8}$$

Multiplying the integral equation, Eq. (19), by $h_k(\beta,\alpha)d\Omega$, integrating, and using the orthogonality condition,

$$\int h_j(\beta,\alpha)h_k(\beta,\alpha)d\Omega = \delta_{jk}\ , \tag{A9}$$

the integral equation can be rewritten in the form

$$g_j(\epsilon)\delta_{jk} = \sum_{n=1}^{\infty}R_{nk}(\epsilon)\varphi_{jn}(\epsilon) \tag{A10}$$

with

$$\begin{aligned} R_{nk}(\epsilon) = {} & \frac{\Omega}{2\pi^2}\frac{(2m_\perp^{*2}m_\parallel^*)^{1/2}}{\hbar^3}\int(\epsilon')^{1/2}\sum_{i=1}^{3}W_i^{\mathrm{int}}(\epsilon,\epsilon')d\epsilon'\delta_{nk} \\ & +\sqrt{\epsilon}\frac{(2m_\perp^{*2}m_\parallel^*)^{1/2}}{4\pi^2\hbar^4}\frac{k_BT}{\rho\bar{v}^2}\int\int(F_1^2+F_2^2+F_3^2)[h_n(\beta,\alpha)-h_n(\beta',\alpha')]h_k(\beta,\alpha)d\Omega\,d\Omega'\ , \end{aligned} \tag{A11}$$

where Eqs. (15) and (11) have been used. $F_l^2(\theta)$ are given by Eqs. (12) and (13). In case the expansions, Eqs. (A8), are restricted to $n = 1,2,3$, the second term of Eq. (A11) can be shown to be of the form

$$\begin{aligned} & \sqrt{\epsilon}\frac{(2m_\perp^{*2}m_\parallel^*)^{1/2}}{4\pi^2\hbar^4}\frac{k_BT}{\rho\bar{v}^2}\int\int(F_1^2+F_2^2+F_3^2)[h_n(\beta,\alpha)-h_n(\beta',\alpha')]h_k(\beta,\alpha)d\Omega\,d\Omega' \\ & \qquad = \frac{1}{\tau_n^{\mathrm{ac}}(\epsilon)}\delta_{nk} \quad \text{for } n = 1,2,3\ . \end{aligned} \tag{A12}$$

Here we have used the group-theoretical argument that the transition probabilities and therefore $F_1^2+F_2^2+F_3^2$ are invariant under the symmetry transformations of the group C_{4v} of $\vec{p}$ space, and therefore the integral is zero except when h_n and h_k transform as the same basis function of an irreducible representation of the group.[46]

Equation (A12) now defines the relaxation times for acoustic phonon scattering $\tau_n^{\mathrm{ac}}(\epsilon)$ for $n = 1,2,3$. Numerical integration of Eq. (A12) gives the relaxation times. For $n = 3$, relating to the $\parallel$ component, one obtains

$$\frac{1}{\tau_\parallel^{\mathrm{ac}}(\epsilon)} = \frac{(m_\parallel^* m_\perp^{*2})^{1/2}\sqrt{2}k_BT\sqrt{\epsilon}}{\hbar^4\rho\pi\bar{v}^2} \times E_d^2\left[1+\xi_\parallel\frac{E_u}{E_d}+\eta_\parallel\frac{E_u^2}{E_d^2}\right] \tag{A13}$$

with the numerical constants

$$\begin{aligned} \xi_\parallel &= 1.62\ , \\ \eta_\parallel &= 1.32\ . \end{aligned} \tag{A14}$$

For $n = 1,2$ relating to the $\perp$ components, the two relaxation times are identical and are given by

$$\frac{1}{\tau_\perp^{\mathrm{ac}}(\epsilon)} = \frac{(m_\parallel^* m_\perp^{*2})^{1/2}\sqrt{2}k_BT\sqrt{\epsilon}}{\hbar^4\rho\pi\bar{v}^2} \times E_d^2\left[1+\xi_\perp\frac{E_u}{E_d}+\eta_\perp\frac{E_u^2}{E_d^2}\right] \tag{A15}$$

with the numerical constants

$$\begin{aligned} \xi_\perp &= 0.83\ , \\ \eta_\perp &= 0.68\ . \end{aligned} \tag{A16}$$

The integration of the first term of Eq. (A11) gives the relaxation times of intervalley phonon scattering, Eq. (24). Equation (A11) may then be written in the form

$$R_{nk}(\epsilon) = \frac{1}{\tau_n(\epsilon)}\delta_{nk} \tag{A17}$$

with [see Eq. (23)]

$$\frac{1}{\bar{\tau}_n(\epsilon)}=\frac{1}{\tau_1^{\rm int}(\epsilon)}+\frac{1}{\tau_2^{\rm int}(\epsilon)}+\frac{1}{\tau_3^{\rm int}(\epsilon)}+\frac{1}{\tau_n^{\rm ac}(\epsilon)}\ . \tag{A18}$$

Inserting Eq. (A17) into Eq. (A10), we get

$$\varphi_{jk}(\epsilon)=\bar{\tau}_k(\epsilon)g_j(\epsilon)\delta_{jk} \tag{A19}$$

and finally

$$\phi_j^0(\vec{\rm p})=\bar{\tau}_j(\epsilon)g_j(\epsilon)h_j(\beta,\alpha) \tag{A20}$$

or

$$\phi_j^0(\vec{\rm k})=-\frac{e}{\hbar}\bar{\tau}_j(\epsilon)[\vec{\nabla}_{\vec{\rm k}}\epsilon(\vec{\rm k})]_j\ , \tag{A21}$$

which is the first of Eqs. (22). Turning now to Eq. (20), the left-hand side of which becomes, by use of Eqs. (A3) and (A20)

$$-\frac{e}{\hbar^2}\Omega_l\phi_j^0(\vec{\rm k})=e\left[\frac{m_l^*}{m_\perp^{*2}m_\parallel^*}\right]^{1/2}\bar{\tau}_j(\epsilon)g_j(\epsilon)h_n(\beta,\alpha)\epsilon_{ljn}\ , \tag{A22}$$

where ϵ_{ljn} is 0, 1, or -1 as defined in Sec. II A 2. Equation (20) is now solved by the same procedure as used to solve Eq. (19) and the result is

$$\phi_{jl}^0(\vec{\rm k})=\frac{e^2}{\hbar m_j^*}\bar{\tau}_j(\epsilon)\bar{\tau}_n(\epsilon)\times[\vec{\nabla}_{\vec{\rm k}}\epsilon(\vec{\rm k})]_n\epsilon_{jln}\ , \tag{A23}$$

which is the second of Eqs. (22).

---

[1] E. H. Putley, *The Hall Effect and Related Phenomena* (Butterworths, London, 1960).

[2] O. Madelung, *Grundlagen der Halbleiterphysik* (Springer, Berlin, 1970).

[3] W. C. Dunlap, Jr., *An Introduction to Semiconductors* (Wiley, New York, 1957).

[4] D. Neubert and R. Schlief, Jahresbericht 1977, Physikalisch Technische Bundesanstalt, Braunschweig, 1978 (unpublished).

[5] J. Messier and J. M. Flores, J. Phys. Chem. Solids 24, 1539 (1963).

[6] A. C. Beer, in *Galvanomagnetic Effects in Semiconductors,* Suppl. 4 of *Solid State Physics,* edited by F. Seitz and D. Turnbull (Academic, New York, 1963).

[7] E. M. Conwell, in *High Field Transport in Semiconductors,* Suppl. 9 of *Solid State Physics,* edited by F. Seitz (Academic, New York, 1967).

[8] D. L. Rode, in *Transport Phenomena,* Vol. 10 of *Semiconductors and Semimetals,* edited by R. K. Willardson and A. C. Beer (Academic, New York, 1975).

[9] J. D. Wiley, in *Transport Phenomena,* Vol. 10 of *Semiconductors and Semimetals,* edited by R. K. Willardson and A. C. Beer (Academic, New York, 1975).

[10] H. F. Wolf, *Silicon Semiconductor Data* (Pergamon, Oxford, 1969).

[11] C. Herring and E. Vogt, Phys. Rev. 101, 944 (1956).

[12] C. Herring, Bell Syst. Tech. J. 2, 237 (1955).

[13] J. Bardeen and W. Shockley, Phys. Rev. 80, 72 (1950).

[14] H. J. G. Meyer, Phys. Rev. 112, 298 (1958).

[15] K. Murase, K. Enjouji, and E. Otsuka, J. Phys. Soc. Jpn. 29, 1248 (1970).

[16] M. Costato and L. Reggiani, Phys. Status Solidi 38, 665 (1970).

[17] J. D. Wiley and M. DiDomenico, Jr., Phys. Rev. B 2, 427 (1970).

[18] W. P. Mason, W. H. Hewitt, and R. F. Wick, J. Appl. Phys. 24, 166 (1953).

[19] B. Lax and J. G. Mavroides, Phys. Rev. 100, 1650 (1955).

[20] Yu. I. Gorkin and K. B. Tolpygo, Fiz. Tverd. Tela (Leningrad) 3, 2903 (1961) [Sov. Phys.—Solid State 3, 2121 (1962)].

[21] G. I. Bir, E. Normantas, and G. E. Picus, Fiz. Tverd. Tela (Leningrad) 4, 1180 (1962) [Sov. Phys.—Solid State 4, 867 (1962)].

[22] A. Hackmann, Diploma thesis, Technical University Berlin, Berlin, 1979 (unpublished).

[23] W. A. Harrison, Phys. Rev. 104, 1281 (1956).

[24] W. P. Dumke, Phys. Rev. 101, 531 (1955).

[25] J. D. Wiley, Solid State Commun. 8, 1865 (1970).

[26] M. Lax and J. J. Hopfield, Phys. Rev. 124, 115 (1961).

[27] M. Lax and J. L. Birman, Phys. Status Solidi B 49, K153 (1972).

[28] H. W. Streitwolf, Phys. Status Solidi 37, K47 (1970).

[29] P. Norton, T. Braggins, and H. Levinstein, Phys. Rev. B 8, 5632 (1973).

[30] B. Fogarassy, Phys. Status Solidi 3, 1646 (1963); 3, 2347 (1963).

[31] E. O. Kane, J. Phys. Chem. Solids 1, 82 (1956).

[32] M. Costato, G. Gagliani, C. Jacoboni, and L. Reggiani, J. Phys. Chem. Solids 35, 1605 (1974).

[33] J. D. Wiley, Phys. Rev. B 4, 2485 (1971).

[34] D. M. Brown and R. Bray, Phys. Rev. 127, 1593 (1962).

[35] E. Ohta and M. Sakata, Jpn. J. Appl. Phys. 17, 1795 (1978).

[36] R. Kubo and T. Nagamiya, *Solid State Physics* (McGraw-Hill, New York, 1969).

[37] R. Schlief, Diploma thesis, Technical University Berlin,

Berlin, 1977 (unpublished).
[38]E. Matsuura, J. Appl. Phys. 33, 1610 (1962).
[39]R. A. Stradling and V. V. Zhukov, Proc. Phys. Soc. London 87, 263 (1966).
[40]G. W. Ludwig and R. L. Watters, Phys. Rev. 101, 1699 (1956).
[41]D. Long, Phys. Rev. 107, 672 (1957).
[42]H. Werner, *Praktische Mathematik I* (Springer, Berlin, 1970).
[43]A. Roizes and R. Schuttler, Phys. Status Solidi A 50, 399 (1978).
[44]R. S. Allgaier, Phys. Rev. B 2, 3869 (1970).
[45]P. Lawaetz, Phys. Rev. 174, 867 (1968).
[46]H. Gabriel and R. Klein, Z. Naturforsch. 19a, 524 (1964).